

Study on Coal Wettability under Different Gas Environments Based on the Adsorption Energy

Published as part of the ACS Omega virtual special issue "CO₂ Geostorage".

Nan Ding, Leilei Si,* Jianping Wei, Wan Jiang, Jian Zhang, and Yong Liu



Cite This: *ACS Omega* 2023, 8, 22211–22222



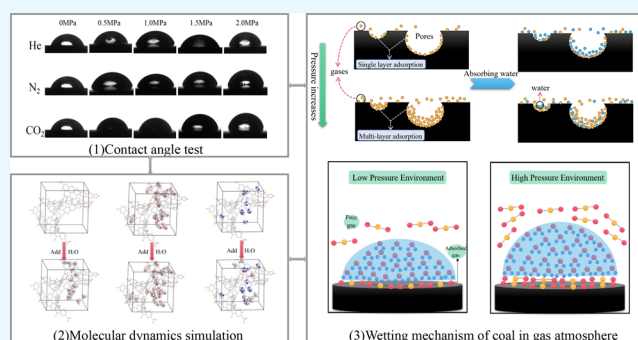
Read Online

ACCESS |

Metrics & More

Article Recommendations

ABSTRACT: Coal seam water injection is a kind of comprehensive prevention and control measure to avoid gas outburst and coal dust disasters. However, the gas adsorbed in the coal seriously influence the coal-water wetting effect. With the deepening of coal seam mining, the gas pressure also gradually increases, but there is still a lack of in-depth understanding of the coal-water wetting characteristics under the high-pressure adsorbed gas environment. Therefore, the mechanism of coal-water contact angle under different gas environments was experimentally investigated. The coal-water adsorption mechanism in pre-adsorbed gas environment was analyzed by molecular dynamics simulation combined with FTIR, XRD, and ¹³C NMR. The results showed that the contact angle in the CO₂ environment increased most significantly, with the contact angle increasing by 17.62° from 63.29° to 80.91°, followed by the contact angle increasing by 10.21° in the N₂ environment. The increase of coal-water contact angle in the He environment is the smallest, which is 8.89°. At the same time, the adsorption capacity of water molecules decreases gradually with increasing gas pressure, and the total system energy decreases after the coal adsorbs gas molecules, leading to a decrease in the coal surface free energy. Therefore, the coal surface structure tends to be stable with rising gas pressure. With the increase in environmental pressure, the interaction between coal and gas molecules enhances. In addition, the adsorptive gas will be adsorbed in the pores of coal in advance, occupying the primary adsorption sites and thus competing with the subsequent water molecules, resulting in a decline of coal wettability. Moreover, the stronger the adsorption capacity of gas, the more obvious the competitive adsorption of gas and liquid, which further weakens the wetting capacity of coal. The research results can provide a theoretical support for improving the wetting effect in coal seam water injection.



1. INTRODUCTION

Coal is the main energy source in China and occupies a dominant position in the energy production and consumption structure. According to statistics, the share of coal consumption in primary energy in China reached 56% in 2021.¹ In addition, coal production and consumption will remain paramount for a longer period of time.

In the process of coal mining, coal dust disaster are major hidden dangers that affect the safety production. The coal seam water injection is a comprehensive measure to eliminate the risk of reducing dust efficiently.^{2,3} When water enters the coal body, the coal seam is wetted, which thus reduces the generation of coal dust during crushing.

Additionally, it can also obstruct gas desorption, thereby decreasing the risk of gas outburst.^{4,5} However, even after gas extraction, there will still be residual gas in the coal seam, which definitely affects the wetting effect of water.⁶ In previous studies, the effects of gas pressure and gas adsorption on the wetting characteristics of coal bodies were mostly ignored.

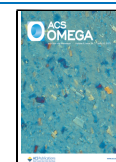
Thus, in order to promote the wetting efficiency of water injection in gas-bearing coal seams, it is especially important to investigate the wetting characteristics of coal under high-pressure gas environments.

Lots of studies have been carried out on the wettability of coal and attributed it to the properties of coal surface and the solution. Cheng et al.⁷ analyzed the relationship between coal wettability and its surface inorganic minerals, finding that the primary minerals represented by quartz among the inorganic minerals are crucial factors to improve the hydrophilicity of coal dust. Furthermore, Li and Li⁸ analyzed the influence of

Received: April 18, 2023

Accepted: May 26, 2023

Published: June 7, 2023



functional groups on the coal wettability by infrared spectroscopy experiments and indicated that oxygen-containing functional groups can effectively improve the hydrophilicity of coal. In addition, many studies have shown that the addition of surfactants can reduce the surface tension of the solution and thus improve the wetting effect of coal seam water injection.^{9,10}

It is well known that the contact angle is a significant index to characterize the wetting properties of coal samples. However, it should be noted that the contact angle is actually a three-phase (solid, liquid, and gas) contact angle. In addition to the property of the coal and solution, the gas condition is also a vital factor affecting the contact angle. Yao and Liu¹¹ investigated the effects of CO₂ and He environment on the wettability of coal by using a low-field NMR test and revealed that the injection of CO₂ into coal could inhibit the water absorption of coal samples, thus reducing the wettability effect, while the injection of He did not change the wettability of coal. Additionally, Chen et al.¹² verified that after coal adsorption of CO₂, the capillary dynamics of water absorption by coal became smaller, thus making the hydrophobicity of coal surface-enhanced and water absorption more difficult. Moreover, the presence of CO₂ changes the environmental pH and the surface charge of coal, making it more hydrophobic.¹³ Similarly, Ibrahim and Nasr-El-Din¹⁴ conducted coal-water contact angle tests at different environmental pressures, showing that the wettability of coal diminishes with increasing pressure, and the contact angle could increase from 61° to 123° when the pressure increased from atmospheric pressure to 13.79 MPa. Wei et al.¹⁵ studied the coal-water contact angle characteristics under different gas environments and verified that the wettability of coal weakens under higher gas pressure conditions. The hydrophobicity of coal under the pre-adsorption CH₄ environment was significantly lower than that under the He environment. The above studies demonstrated that coal-water wettability has a crucial relationship with the gas environment, and it is generally accepted that coal-water wettability decreases with the increase of environmental pressure. However, coal is a naturally porous medium, and its complex internal pore structure provides space for gas and liquid adsorption. Its unique adsorption characteristics have an essential influence on coal-water wetting, especially for the wetting characteristics of gas-bearing coal. Most of the existing studies attribute the changes in the wetting features of gas-bearing coal to the effect of environmental pressure, ignoring the adsorption of gas, so it is still necessary to explore the wettability of coal in different adsorptive gas environments.

In summary, a contact angle test system under controlled temperature and pressure conditions was constructed to investigate the variation law of coal-water contact angle in various gas environments. Then, XRD, FTIR, and ¹³C NMR were performed on the coal samples to analyze their physicochemical properties. Additionally, the macromolecular model of the coal sample was constructed to explore the microscopic coal-water interaction characteristics under different gas environments by molecular dynamics simulation. The results can provide theoretical support for improving the wetting effect of water injection in gas-bearing coal.

2. EXPERIMENTAL METHODS

First, the contact angle was measured in CO₂, N₂, and He environments (pressure 0–2 MPa). Then, XRD, FTIR, and ¹³C NMR were used to obtain the mineral composition,

functional group structure, and carbon atom information of coal samples. The molecular dynamics simulations were performed to reveal the coal-water adsorption processes in different gas environments, so as to obtain microscopic parameters, such as adsorption amount, adsorption energy, and interaction energy of coal on each adsorbent under different gas environments. The experimental procedure is shown in Figure 1.

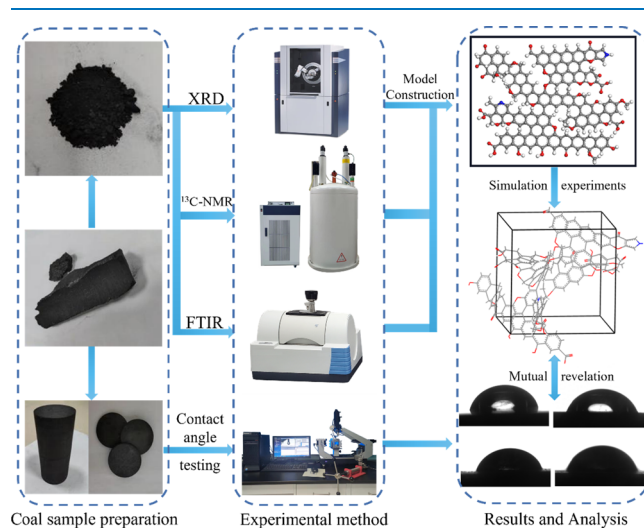


Figure 1. Experimental flow chart of coal-water contact characteristics under different gas environments.

2.1. Sampling. The experimental sample (SP) was processed for subsequent testing. Some samples were cut into circular slices of $\varphi 50 \times 3$ mm, and the surface of the coal samples were polished smooth for contact angle test. The coal powder was used for proximate analysis, elemental analysis, XRD, FTIR and ¹³C NMR. The basic parameters of SP coal are shown in Table 1.

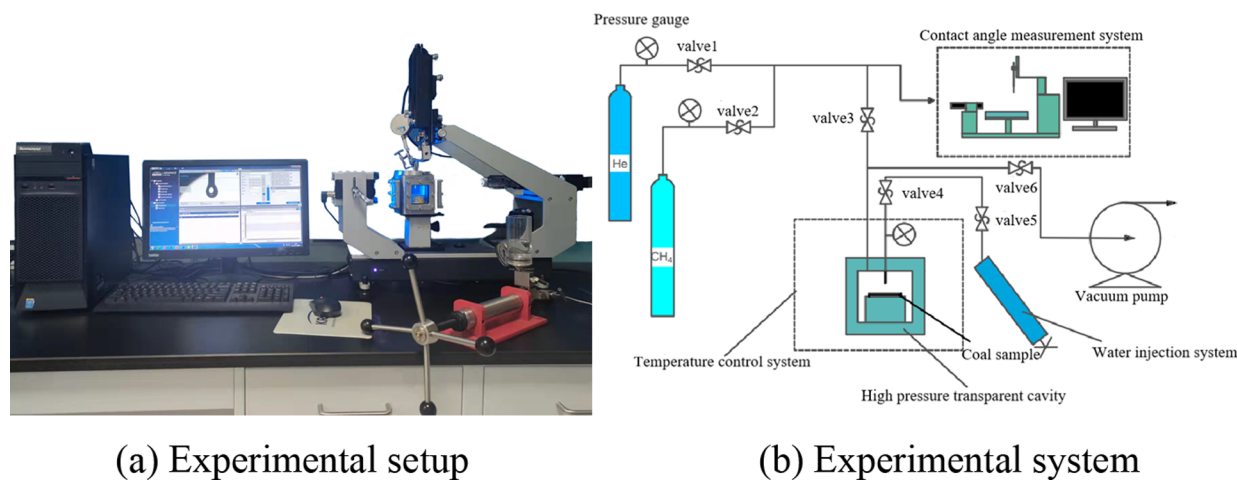
2.2. Coal-Water Contact Angle Experiments in Different Gas Environments. An experimental system that can realize the coal-water contact angle measured in different environments was built. As shown in Figure 2, the device is mainly composed of an HD camera, a transparent gas canister, a water injection device, and a computer. The experimental procedure is as follows:

- (1) 0.5 MPa He is injected into the chamber and sealed, and the gas tightness is ensured by observing whether the pressure changes. Then, the sample is placed into the gas canister and degassed under vacuum to exclude the residual gas inside the canister and the coal pores.
- (2) Connect the gas injection device, fill the high-pressure transparent chamber with gas at a preset pressure, and then close the chamber and place it in a constant temperature environment for 6–8 h (all experimental temperatures in this paper are 30 °C).
- (3) When the fluctuation of the pressure sensor value is less than 0.05 MPa within 30 min, turn on the computer and adjust the sample to the proper position.
- (4) A drop of distilled water is slowly applied to the sample; then, the contact angle is measured by the software and the data are saved.
- (5) Change the experimental gas conditions and repeat the operation (1) to (5). In this paper, the experimental

Table 1. Proximate Analysis and Elemental Analysis of SP Coal Sample^a

coal sample	proximate analysis/%				elemental analysis/%				
	M_{ad}	A_{ad}	V_{ad}	FC_{ad}	C	H	O	N	S
SP	1.18	13.67	8.13	77.02	75.00	3.218	20.205	0.98	0.597

^aNotes: M_{ad} : moisture content; A_{ad} : ash content; V_{ad} : volatile content; FC_{ad} : fixed carbon content.

**(a) Experimental setup****(b) Experimental system****Figure 2.** Diagram of coal-water contact angle test apparatus.**Table 2. Molecular Dynamics Simulation Scheme**

number	simulation scheme	inducing factors
constant pressure adsorption	scheme 1 coal molecules adsorb CO ₂ gas molecules to a preset pressure (0–2 MPa), and then quantitatively adsorb water molecules	adsorption volume, adsorption energy, equivalent heat of adsorption, and ambient pressure
	scheme 2 coal molecules adsorb N ₂ gas molecules to a preset pressure (0–2 MPa), and then quantitatively adsorb water molecules.	
	scheme 3 coal molecules adsorb He gas molecules to preset pressure (0–2 MPa), then quantitatively adsorb water molecules	
saturation adsorption	scheme 4 adsorption of water molecules by coal molecules to saturation (control group)	adsorbent, saturated adsorption capacity
	scheme 5 coal molecules first adsorb CO ₂ gas molecules to saturation and then water molecules to saturation	
	scheme 6 coal molecules first adsorb N ₂ gas molecules to saturation and then water molecules to saturation	

gases are CO₂, N₂, and He, and the gas pressure is 0–2.0 MPa.

2.3. ¹³C NMR Test. In order to model the macromolecular structure of coal, information on the carbon atoms of the coal sample is needed. The ¹³C NMR experiments were performed on Bruker Avance 600 M solid-state NMR spectrometer. The experiments were performed with a 4 mm dual resonance MAS probe, a rotor operating speed of 10 kHz, a pulse width of 20 μs, and a pulse delay time of 2 s. The resonance frequency of the ¹³C detection nucleus was 150.99 MHz, the sampling time 0.0344 s, and the number of scans was 4800.

2.4. FTIR Test. To obtain the composition of each organic functional group in coal molecules and to analyze the effect of functional groups on coal wettability, the infrared spectra of coal samples were measured by Nicolet iS50 FTIR infrared spectrometer. The samples were dried in a vacuum drying oven at 60 °C for 60 min before the test. Then, 200 mg of potassium bromide was taken as the carrier, and the coal sample and potassium bromide were mixed and ground at a ratio of 1:100. Eventually, the samples were pressed on a tablet press into thin slices of 13 mm diameter and 0.1 to 1 mm thickness. In this experiment, the infrared spectrum was scanned in the range of 400–4000 cm⁻¹, with 64 scans and a resolution of 4 cm⁻¹.

2.5. XRD Test. To analyze the mineral composition and microcrystalline structure information of coal samples, XRD tests were performed on coal samples using a Bruker D8 Advance X-ray diffractometer with the following experimental conditions: Cu target radiation ($\lambda = 0.15418$ nm), scan range 5–80°, tube voltage = 40 kV, tube current = 40 mA, step size 0.02°, and a test speed 0.1 s/step.

2.6. Molecular Dynamics Simulation. Molecular dynamics simulations were designed for two sets of scenarios: constant pressure adsorption and saturation adsorption. The process of constant pressure adsorption simulation is to make SP coal molecules adsorb different gas molecules to the preset pressure, respectively, and then quantitatively adsorb H₂O molecules to analyze the adsorption capacity of coal to different gases in different conditions. Saturation adsorption is to add gas molecules to coal molecules one by one until the system energy is reduced to a minimum, and it is determined as the saturation state of gas adsorption. Then, H₂O molecules are added to coal molecules in this state until the adsorption is saturated with H₂O. The He group is no longer set for saturation adsorption because of its non-adsorption ability, and the specific experimental scheme is shown in Table 2.

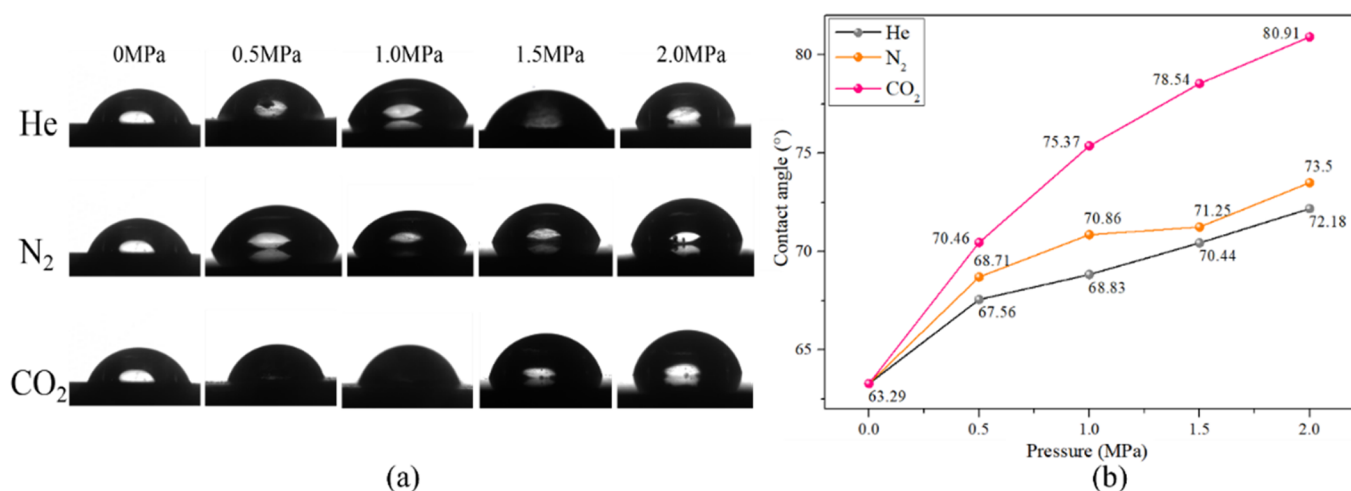


Figure 3. Test results of coal-water contact angle under different gas pressures.

The constant pressure and saturation adsorption simulations were performed under the fixed pressure and locate functions in the Sorption module, respectively. The simulation experiments were performed by using the GCMC (Giant Canonical Monte Carlo) method, with the Metropolis-focused sampling method selected as the calculation method. The adsorption simulation was performed under the COMPASS II force field, the charge calculation was selected from Forcefield assigned. The summation methods of electrostatic interaction and van der Waals interaction were adopted from Ewald & Group and Atom-based, respectively.

3. RESULTS AND ANALYSIS

3.1. Variation of Coal-Water Contact Angle in Different Gas Environments. The coal-water contact angle tests of SP coal in CO₂, N₂, and He environments is shown in Figure 3. In the CO₂ environment, the contact angle increased from 63.29° to 80.91° with the pressure ranging from 0 to 2 MPa. Similarly, the contact angle increased from 63.29° to 73.50° and 72.18° with increasing pressure in the N₂ and He environments, respectively. In summary, the contact angle always increases with increasing pressure, and the most significant increase was in the CO₂ environment, while the contact angle changed the least in the He environment. The increase in contact angle implies a weakening of coal wettability.^{16,17} Preliminary analysis suggests that in CO₂ and N₂ environments, the coal-water contact angle is affected by both gas adsorption and gas pressure and therefore changes more significantly compared to He because coal adsorbs CO₂ and N₂. Additionally, the contact angle increase differs due to the difference in coal's ability to adsorb the two gases. In contrast, due to the non-adsorptive nature of He, the contact angle in the He environment is only influenced by the pressure, and the contact angle increase is minimal.

3.2. ¹³C NMR Test Results. The main component of coal is elemental carbon, and the form of carbon atoms present in coal is of great significance to study the properties of coal samples and the construction of coal macromolecule structure. Figure 4 shows the ¹³C NMR split-peak fitted spectra of SP coal sample. There are three obvious carbon peaks in the coal sample, which are the fatty carbon peak located at 50–80 ppm, the aromatic carbon at 100–150 ppm, and the carbonyl and carboxyl peaks at 175–220 ppm. Among them, methoxy at 59

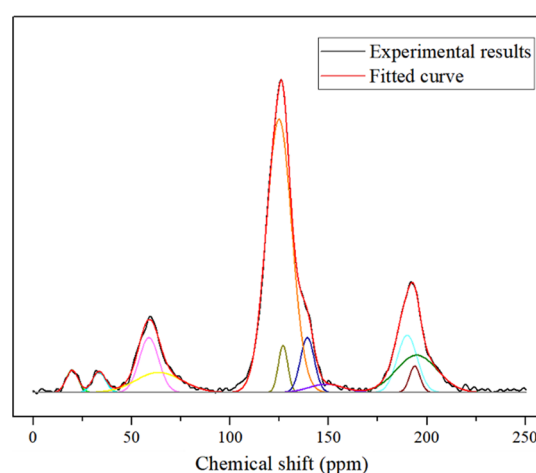


Figure 4. ¹³C NMR peak fitting spectrum of coal sample.

ppm was the dominant peak in the lipid carbon region, and protonated aromatic carbon at 125 ppm was the dominant peak in the aromatic carbon region. Combined with ¹³C NMR carbon atom chemical shift attribution, the absorption peak parameters, such as peak position and relative content of each functional group of SP coal samples, are listed in Table 3. Meanwhile, the structural parameters of SP can be calculated in Table 4. The data show that the aromatic carbon (f_a')

Table 3. Structure Parameters of ¹³C NMR Peak Fitting of Coal Sample

number	peak position	half-peak width	relative area	carbon atom attribution
1	19.82	7.18	1.91	Ar-CH ₃
2	33.41	7.81	1.92	CH ₂
3	58.82	11.68	7.68	O-CH ₃ , O-CH ₂
4	63.78	27.35	6.58	O-CH
5	124.85	15.29	50.17	Ar-H
6	126.91	5.55	3.13	Ar-H
7	139.26	8.27	5.44	Ar-C
8	148.79	20.13	1.99	Ar-O
9	189.97	11.99	8.21	CCOOH
10	193.77	6.36	1.99	C=O
11	194.79	24.53	10.96	C=O

Table 4. Structural Parameters of SP Coal^a

coal sample	f_a	f_a^C	f_a'	f_a^N	f_a^H	f_a^P	f_a^S	f_a^B	f_a^I	f_a^{I*}	f_{al}^H	f_{al}^O
SP	83.29	20.79	62.50	35.08	41.25	0.70	6.26	14.05	16.71	1.25	2.64	12.82

^aNotes: f_a – total sp² heterocarbon; f_a^I – total sp³ heterocarbon; f_a^C – carbonyl (carboxy) carbon; f_a' – aromatic carbon; f_a^H – protonated aromatic carbon; f_a^N – non-protonated aromatic carbon; f_a^P – oxygenated aromatic carbon; f_a^S – lipid-substituted aromatic carbon; f_a^B – bridged aromatic carbon; f_{al}^H – non-methyl carbon; f_a^{I*} – methyl carbon; f_{al}^O – oxygenated lipid carbon.

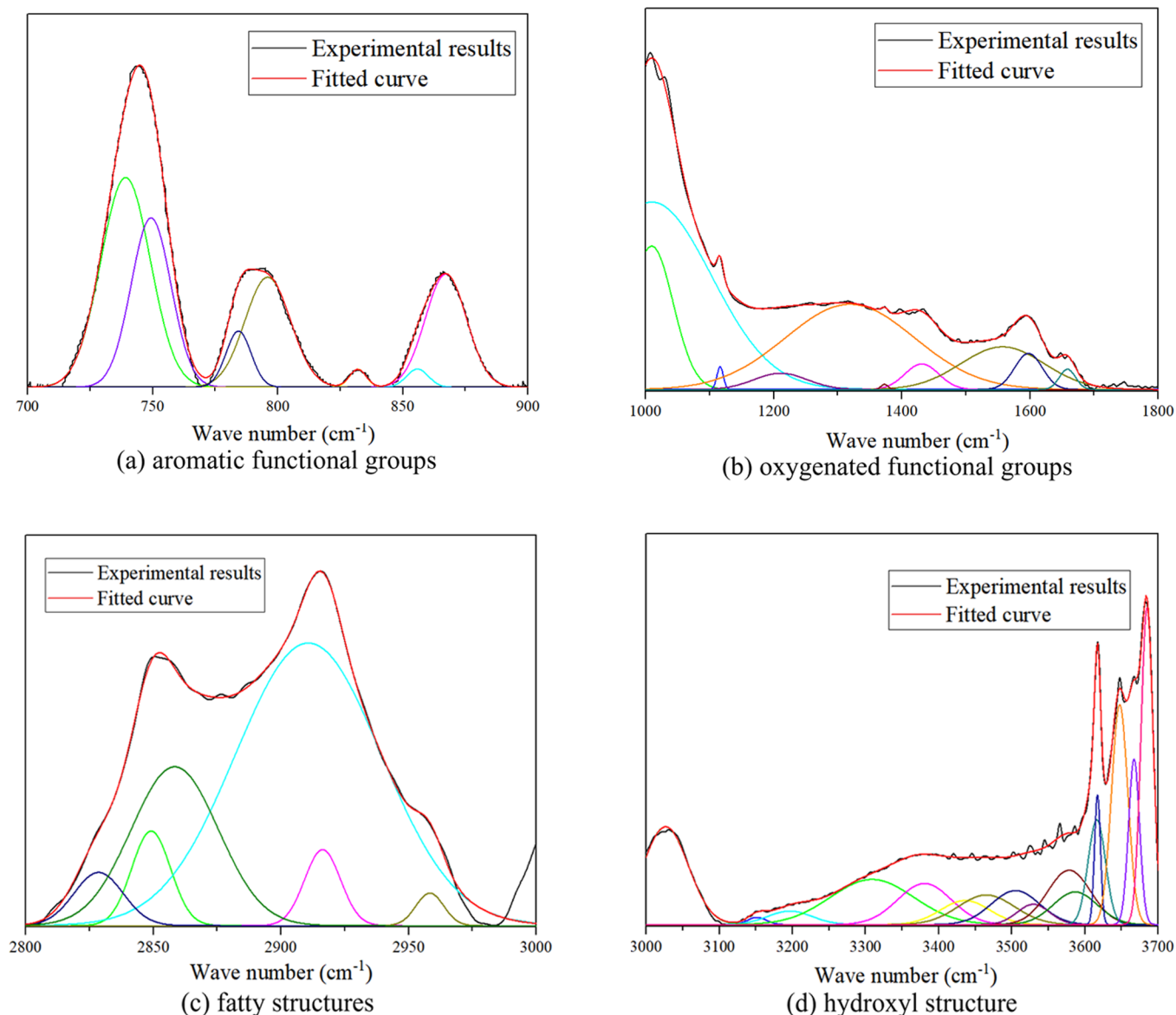


Figure 5. FTIR fitting spectra of coal sample.

structure is the main component of SP coal molecules, with the relative content accounting for 62.50%. Then, the carbonyl and carboxyl (f_a^C) accounted for 20.79%, and aliphatic carbon (f_{al}) accounted for 16.71%. In addition, the aromatic bridge carbon to perimeter carbon ratio (X_{BP}) is a vital parameter to reflect the degree of aromatic ring condensation of coal samples, and the ratio of bridge carbon to perimeter carbon of SP coal samples is calculated to be 0.291 according to eq 1.

$$X_{BP} = \frac{f_a^B}{f_a^H + f_a^P + f_a^S} \quad (1)$$

3.3. FTIR Test Results. FTIR can reflect the presence of functional groups in coal. Figure 5 shows the spectra of the SP coal sample in each band and the results of peak fitting. The FTIR spectra are divided into four parts according to the different types of functional groups: aromatic functional groups at 700–900 cm⁻¹ (Figure 5a), oxygenated functional groups at 1000–1800 cm⁻¹ (Figure 5b), fatty structures at 2800–3000 cm⁻¹ (Figure 5c) and hydroxyl structure at 3000–3800 cm⁻¹ (Figure 5d). The absorption peak parameters and attribution of each waveband are shown in Tables S678. The results indicated that the benzene ring in the aromatic functional group of the SP coal sample is mainly substituted with the benzene ring binary, accounting for 59.21%. The oxygen-

Table 5. Infrared Fitting Parameters of Aromatic Structure

number	peak position	half-peak width	relative area	attribution
1	739.14	23.31	35.87	disubstituted aromatics
2	749.31	18.77	23.33	disubstituted aromatics
3	784.28	11.81	4.87	trisubstituted aromatics
4	795.95	21.45	17.32	trisubstituted aromatics
5	831.94	7.86	1.04	tetrasubstituted aromatics
6	855.81	10.28	1.38	tetrasubstituted aromatics
7	867.17	19.46	16.18	pentasubstituted aromatics

Table 6. Infrared Fitting Parameters of Oxygen-Containing Functional Groups Structure

number	peak position	half-peak width	relative area	attribution
1	1009.61	219.65	35.95	ash
2	1010.55	78.49	11.09	ash
3	1116.32	11.76	0.43	C–O expansion
4	1210.64	97.81	2.57	C–O expansion
5	1318.95	237.51	32.74	C–O expansion
6	1372.85	13.04	0.11	CH ₂ symmetric
7	1431.06	62.37	2.57	CH ₃ , CH ₂
8	1556.92	153.37	10.59	C=C vibration
9	1597.45	50.55	2.95	C=C vibration
10	1658.23	29.86	0.98	C=O vibration

Table 7. Infrared Fitting Parameters of Aliphatic Hydrocarbons Structure

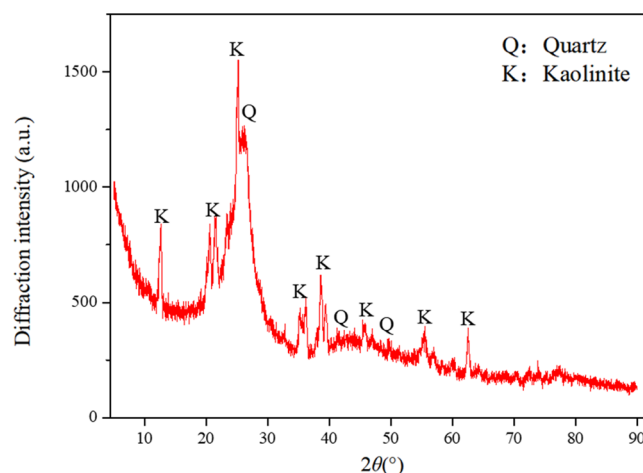
number	peak position	half-peak width	relative area	attribution
1	2828.53	22.75	4.03	CH ₂ symmetric scaling
2	2849.11	17.97	5.67	CH ₂ symmetric scaling
3	2858.36	40.16	21.29	CH ₃ symmetric scaling
4	2910.71	67.26	63.39	CH asymmetric expansion
5	2916.25	16.64	4.21	CH ₂ does not stretch

Table 8. Infrared Fitting Parameters of Hydroxyl Structure

number	peak position	half-peak width	relative area	attribution
1	3026.45	73.01	11.55	aromatic ring C–H stretching
2	3151.32	30.29	0.44	cyclic hydroxyl hydrogen bonding
3	3196.52	71.14	1.93	cyclic hydroxyl hydrogen bonding
4	3308.82	134.03	12.16	hydroxy-ether hydrogen bond
5	3380.43	86.58	7.14	self-conjugated hydroxyl hydrogen bonds
6	3436.05	79.49	3.83	self-conjugated hydroxyl hydrogen bonds
7	3464.98	90.92	5.39	self-conjugated hydroxyl hydrogen bonds
8	3504.89	77.99	5.32	hydroxy- π -hydrogen bond
9	3529.28	52.43	2.13	hydroxy- π -hydrogen bond
10	3578.28	69.78	7.61	hydroxy- π -hydrogen bond
11	3586.55	71.22	4.66	hydroxy- π -hydrogen bond
12	3616.01	27.99	5.88	free hydroxyl group
13	3616.96	9.57	2.49	free hydroxyl group
14	3647.27	26.15	11.54	free hydroxyl group
15	3666.90	17.59	5.84	free hydroxyl group

containing functional groups in the SP coal sample exist in the form of carbonyl, hydroxyl, and ether oxygen, while there are almost no carboxyl groups due to their high degree of metamorphism. In addition, the aliphatic carbon in coal is mainly in the form of branched chains or linked aromatic rings, such as aliphatic rings, side chains, or bridging carbon.¹⁸ Eventually, the results show that the coal samples have the largest proportion of free hydroxyl groups, followed by hydroxyl- π hydrogen bonds and self-conjugated hydroxyl hydrogen bonds. Functional groups are principal factors affecting the wettability of coal, and it is generally accepted that coal contains oxygen functional groups, such as hydroxyl, carboxyl, phenolic hydroxyl, and other polar state functional groups. Due to their strong polarity, can join with the hydrogen of water molecules in the form of hydrogen bonds by dipolar force to enhance the hydrophilicity of coal.¹⁹ In summary, the hydrophilic functional groups, such as hydroxyl groups and other oxygen-containing functional groups are more abundant in the SP coal sample. Therefore, this sample is considered to have good wettability, and the results of FTIR spectrum fitting lay the foundation for the construction of coal sample macromolecules.

3.4. XRD Test Results. XRD is widely used to test the types and contents of inorganic minerals in coal, and it can also be used to characterize the structural features of coal aggregates and reveal the structural composition of coal macromolecules. Figure 6 shows the XRD spectrum of the SP

**Figure 6.** XRD spectrum of coal sample.

coal. The physical phase analysis of the inorganic mineral composition of the coal samples revealed that the minerals in the SP coal were dominated by kaolinite and quartz. These two kinds of inorganic substances formed by Si element in different coal-forming periods can effectively promote the wettability of coal,²⁰ so the high content of inorganic mineral components in coal samples is one of the reasons for their better wettability. Meanwhile, two peaks can be clearly observed in the spectrum, located around 25° and 45°. They represent the peaks generated by the 002 and 100 crystal planes, respectively. The 002 peak includes the 002 band and the γ band, which are the result of the joint action of both. The 002 band is related to the stacking nature of the aromatic structure, while the γ band is mainly formed due to the presence of branched micro-crystals. Furthermore, the formation of the 100 peak is mainly related to the degree of condensation of the aromatic ring.

According to the Bragg equation and Scheele's formula (eqs 2–5),²¹ the aromatic layer spacing (d_{002}), the aromatic layer sheet stacking height (L_c), and the planar ductility of the aromatic layer (L_a) of SP coal were calculated for the subsequent SP coal macromolecular model construction. The relevant parameters are shown in Table 9.

$$d_{002} = \frac{\lambda}{2\sin \theta_{002}} \quad (2)$$

$$L_c = \frac{K_c \times \lambda}{\beta_{002} \cos \theta_{002}} \quad (3)$$

$$L_a = \frac{K_a \times \lambda}{\beta_{100} \cos \theta_{100}} \quad (4)$$

$$N_{ave} = \frac{L_c}{d_{002}} \quad (5)$$

Table 9. Microcrystalline Structure Parameters of Coal Sample

coal sample	d_{002}/nm	L_c/nm	L_a/nm	N_{ave}
SP	0.34	1.83	2.01	5.33

where λ is the wavelength of X-rays, 0.15406 nm. θ_{002} and θ_{100} correspond to the diffraction angles of the 002 and 100 peaks, and β_{002} and β_{100} correspond to the half-peak widths of the 002 and 100 peaks, respectively. K_c and K_a are the microcrystalline shape factors of coal dust, $K_c = 0.89$, $K_a = 1.84$, and N_{ave} is the number of aromatic layers of coal molecules.

3.5. Molecular Dynamics Simulation Results.

3.5.1. Modeling of coal samples. Based on the elemental analysis results, the molecular formula of coal samples was initially estimated to be $C_{179}H_{92}O_{36}N_2$ using the mathematical equation assumption method. Then the number of aromatic carbon f_a' could be calculated as 112 from the results of ^{13}C NMR experiments. According to the X_{BP} value of the coal sample, it is known that the macromolecular structure of the SP coal sample is dominated by naphthalene and anthracene (phenanthrene) and supplemented by benzene and pyrene rings. The number of aromatic rings, such as benzene ring, naphthalene ring, and anthracene ring in the coal molecular configuration was adjusted to make the bridge-carbon ratio close to the calculated value. Then, the aromatic forms and numbers of SP coal samples were obtained, as shown in Table 10. Finally, combined with the results of FTIR spectra fitting in

the previous section, the number, and structures of each atom were adjusted to determine the chemical molecular formula of the SP coal samples was determined as $C_{175}H_{96}O_{36}N_2$. The planar model of the coal sample macromolecule was drawn by Visualizer module of Materials Studio software, as shown in Figure 7a. Then the structure was optimized and annealed to obtain a structurally stable molecular model and adding periodic boundaries to an SP coal molecule by Amorphous Cell. The model was then optimized for density from 0.5 to 1.5 g/cm^3 , as shown in Figure 7b, thus determining the coal molecular density to be 1.2 g/cm^3 . The final structurally stable three-dimensional configuration of the coal molecule shown in Figure 7c was obtained and used in the subsequent simulation experiments.

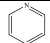
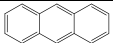
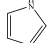
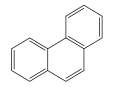
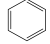
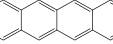
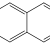
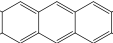
3.5.2. Adsorption simulation experiment results. Figure 8 shows the simulation results of schemes 1–3, modeling the process of adsorption of water molecules in different gas environments. Figure 9 shows the adsorption capacity of each gas by coal in different conditions.

The presence of lots of pores in coal makes it have a high surface free energy.^{22,23} According to the principle that the lower the energy, the more stable the system is. Coal pores will continuously adsorb various tiny substances around to lower the surface free energy, such as gas, water, etc.²⁴

The constant pressure adsorption models (Figures 8 and 10) show that with the increase of gas pressure, the adsorption of coal on gas molecules increases from 32.10 moles/u.c. at 0.5 MPa to 36.81 moles/u.c. at 2 MPa for the CO_2 environment. and the adsorption of coal on gas molecules increases from 12.23 moles/u.c. at 0.5 MPa to 23.19 moles/u.c. at 2 MPa for the N_2 environment, while almost no adsorption on the He environment. The gas adsorption gradually increases, which is shown in the model diagram as a gradual aggregation of red areas in the pores of coal molecules and an increase in area and density. The magnitude of the equivalent heat of adsorption of coal on gas can indirectly reflect the capacity of coal surface to adsorb gas. The simulation results show that the equivalent heat of adsorption of CO_2 and N_2 by coal is 37.63 and 18.52 KJ/mol , respectively.

To discover the wettability of the SP coal molecules after pre-sorption of different pressure gases, the adsorption energy between coal samples and each adsorbent in different gas environments was calculated. The results are shown in Figure 10, where the curves in Figure 10a show the adsorption energy data of coal for different gases during constant pressure adsorption. Figure 10b shows the adsorption energy results of coal samples for the quantitative adsorption of 5 H_2O

Table 10. Type and Quantity of Aromatic Structure in Coal Samples

type	quantity	type	quantity
	1		2
	1		1
	1		1
	3		1

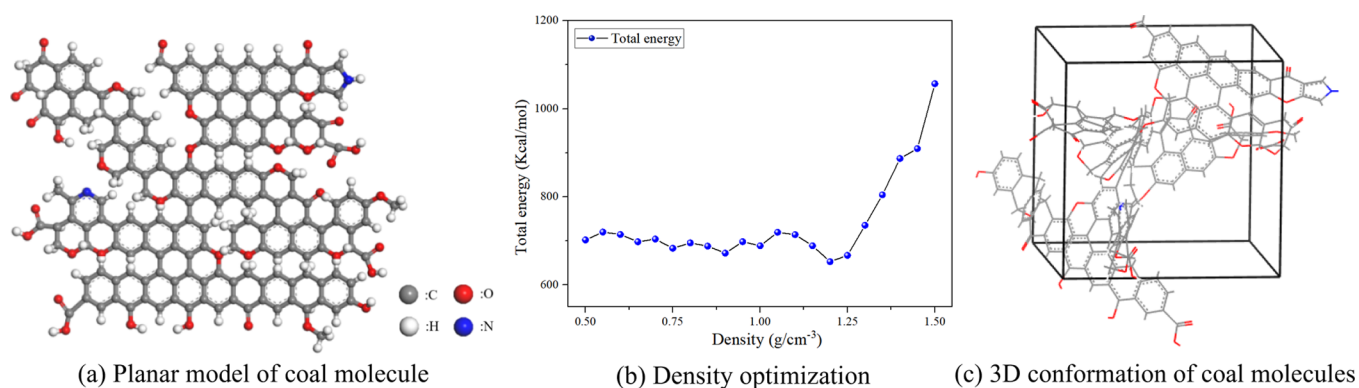


Figure 7. Construction and optimization of macromolecular structure model of SP coal sample.

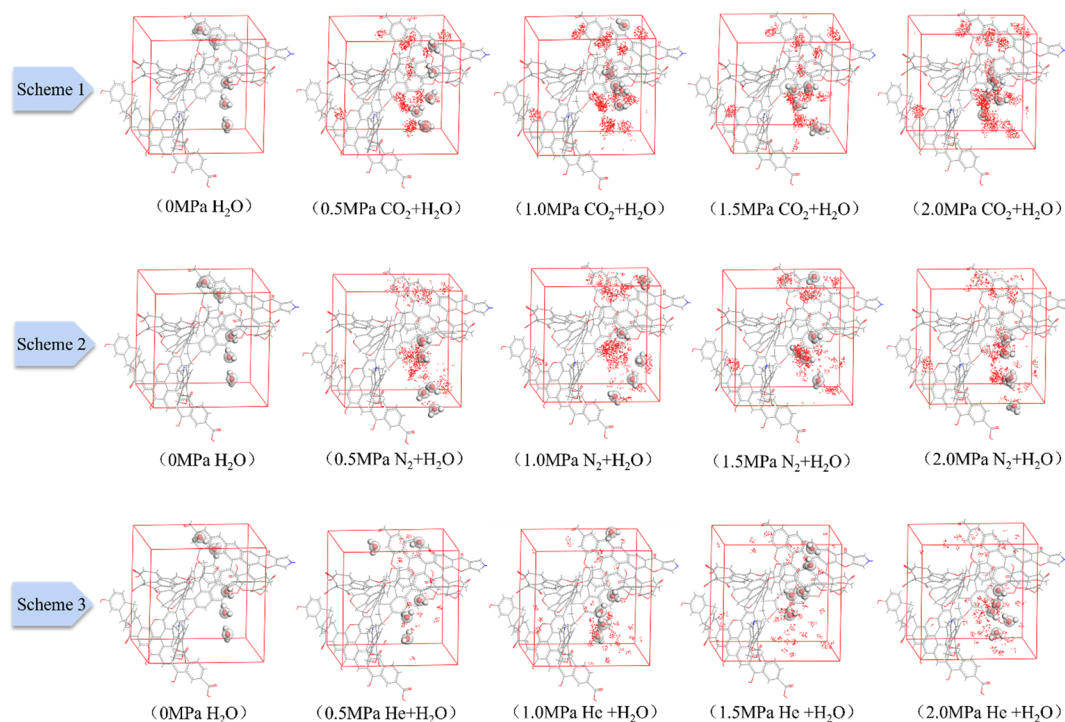


Figure 8. Molecular models of coal adsorbing water under different gas environments.

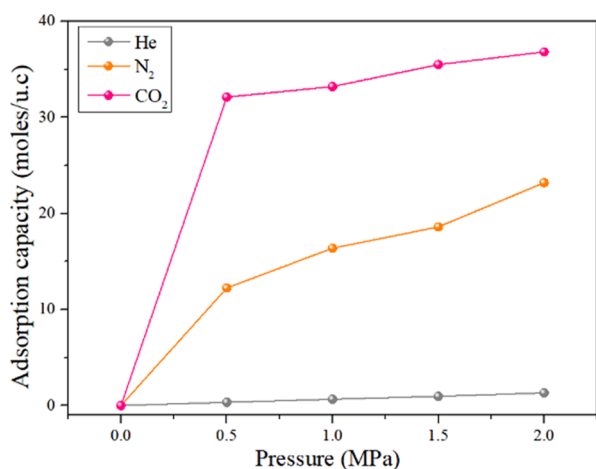


Figure 9. Change curve of coal adsorption capacity for gas under different gas pressure.

molecules under different gas environments. The negative value of adsorption energy here indicates that the adsorption is an exothermic reaction and the energy of the system decreases. While the smaller value of adsorption energy indicates that the energy of the system decreases more, and the system is more stable. So, it can be considered that the smaller value of adsorption energy indicates that the adsorption behavior is more likely to occur, i.e., the better wettability of the coal. The data in the figure show that as the environmental pressure increases, the gas molecules adsorbed on the pore surface of coal gradually increase. It makes the carbon atoms on the coal surface tend to be in equilibrium and thus reduces the free energy on the coal surface. Therefore, after the coal adsorbed with gas molecules is exposed to water again, the attraction ability for H₂O molecules is reduced compared with that without the influence of gas adsorption (i.e., He environment). This is identified as an important cause of the deterioration of coal wettability. In contrast, the calculation results still gradually increase for the non-adsorbed He environment. In

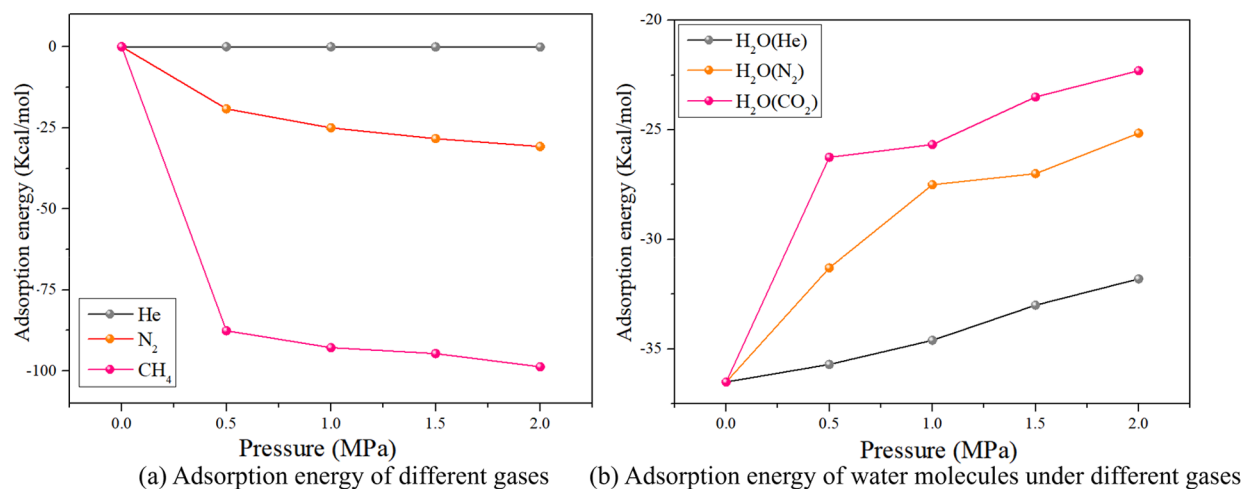


Figure 10. Variation of adsorption energy of coal sample for each adsorbent under different gas environments.

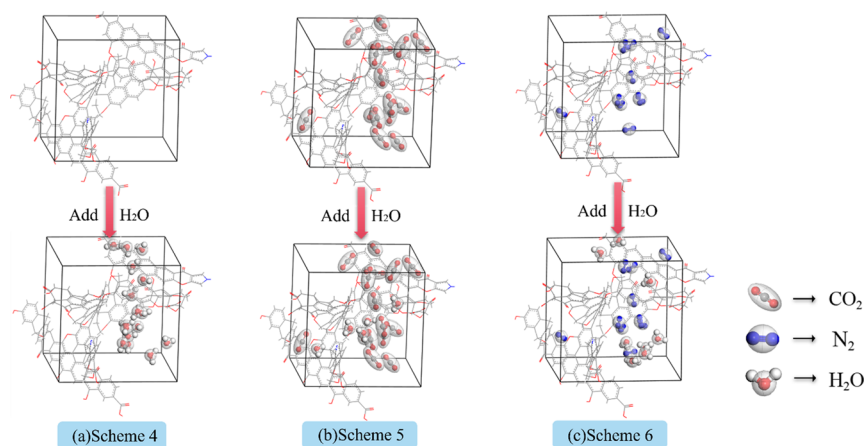


Figure 11. Saturation adsorption model of coal on different gas and water molecules.

this case, it is mainly due to the influence of environmental pressure, which will be analyzed in detail later.

Figure 11 shows the results of saturation adsorption experiments. Figure 11a shows the adsorption configuration of the SP coal molecules when water molecules are adsorbed to saturation. Besides, Figure 11b,c shows the adsorption configurations of coal molecules when CO₂ and N₂ are adsorbed to saturation, and then water molecules are added to saturation one by one, respectively. The results show that the coal sample was saturated with 15 H₂O, 15 CO₂, and 10 N₂ adsorbed separately. However, when the coal sample was pre-adsorbed with gas molecules, only 5 and 9 H₂O molecules are needed to reach saturation, respectively. Meanwhile, the adsorption state of each adsorbent molecule in the pores of coal molecules was observed. It shows that when H₂O molecules were added one by one, the H₂O molecules were firstly adsorbed near the oxygen-containing functional groups such as the hydroxyl and ether bonds of the coal sample. Additionally, as the number of H₂O molecules increased, they were adsorbed in the pores of coal from outside to inside. At the same time, the adsorption sites of H₂O molecules were gradually shifted from coal molecules to the adsorbed H₂O molecules. This result is consistent with the conclusion of the study by Jin et al.²⁵ The hydrogen bonding energy between the O atoms of the hydrophilic functional groups of coal molecules and the H atoms of H₂O molecules is the main reason for the

primary adsorption sites of H₂O molecules. With the increase of adsorption amount, the multi-molecular layer adsorption was produced because of the stronger adsorption of CO₂. So, the effect of inhibiting wettability of coal by CO₂ far exceeded the effect of N₂ atmosphere.^{26,27} In summary, when the aqueous solution wets the coal sample containing gas adsorption, the water molecules will compete with the gas molecules for adsorption. Thus, resulting in fewer water molecule adsorption sites, lower adsorption, and weaker wettability.

4. DISCUSSION

4.1. Gas–Liquid Competitive Adsorption. Many studies were conducted about the competitive adsorption mechanism of gas–liquid in coal pores. These studies are primarily focused on explaining the situation, where the gas and liquid are adsorbed at the same time.²⁸ However, in the actual coal seam water injection process, gas has been preferentially present in the pore of coal seam with adsorption and free state.²⁹ However, the pre-adsorbed gas in the coal seam will inevitably influence the wetting effect of water injection.

However, according to the saturated competitive adsorption simulation results shown in Figure 11, the pre-adsorbed gas molecules will preferentially occupy the primary adsorption sites and reduce the surface free energy of the coal to make the system more stable.^{30,31} When the water molecules are

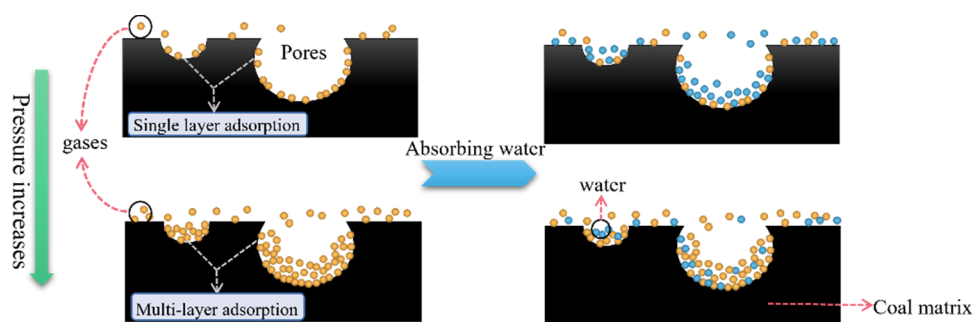


Figure 12. Gas–liquid competitive adsorption mechanism on coal pore surface.

adsorbed later, gas and water will compete to be adsorbed due to the limited adsorption sites. Therefore, the water molecules need more energy to get inside the coal body, making the contact angle increase. Figure 12 shows the mechanism of gas–liquid competitive adsorption on the pore surface of coal. In the gas environment, the gas adsorption gradually changes from monolayer adsorption to multilayer adsorption with the increasing gas pressure. As the adsorption sites are occupied by gas molecules in advance, the water molecules will seize the adsorption sites along with the desorption of gas molecules. Therefore, the presence of pre-adsorbed gas in the coal seam will compete with the water molecules. The stronger the gas adsorption capacity, the greater the impact on the adsorption of water molecules, resulting in the deterioration of coal wettability.

4.2. Effect of Environmental Pressure on the Wettability of Coal. The above experimental results and extensive studies have shown that environmental pressure is one of the main factors affecting the wettability of coal. For the adsorptive gases CO_2 and N_2 , the density of gas molecules in the coal pores increases as the pressure grows. It also enhances the probability of gas contact with the pore surface of the coal sample.^{32,33} Thereby, the gases are more readily adsorbed by coal, causing an increase in the adsorption amount.^{34,35} To further verify the effect of increased gas pressure on coal wettability, the interaction energy between adsorbed gas molecules and coal molecules under different gas pressure environments was calculated by eq 6.

$$E_{\text{int}} = E_{\text{total}} - E_{\text{surface}} - E_{\text{adsorbate}} \quad (6)$$

where E_{int} is the coal–gas interaction energy, E_{total} is the total system energy, E_{surface} is the coal molecular surface energy, and $E_{\text{adsorbate}}$ is the energy of the adsorbent gas molecular system.

The results of the interaction energy calculations of the SP coal molecules with adsorptive gas molecules at different pressures are shown in Figure 13. As the pressure increases from 0.5 to 2 MPa, the interaction energy of coal with CO_2 and N_2 both decreases. The smaller interaction energy represents a lower system energy and a more stable surface system. Therefore, the results indicate that the increase in environment pressure enhances the binding ability of the adsorbed gas to the coal. It also results an increase in the energy required for the H_2O molecule to replace the gas adsorbed on the coal surface, which leads to a weakening of coal wettability.

It is well known that the capillarity of the coal pores plays an essential role in the absorption of the water. For the non-adsorptive gas He, it exists mainly in the free form in the fissures of coal. Therefore, as the pressure rises, the free gas

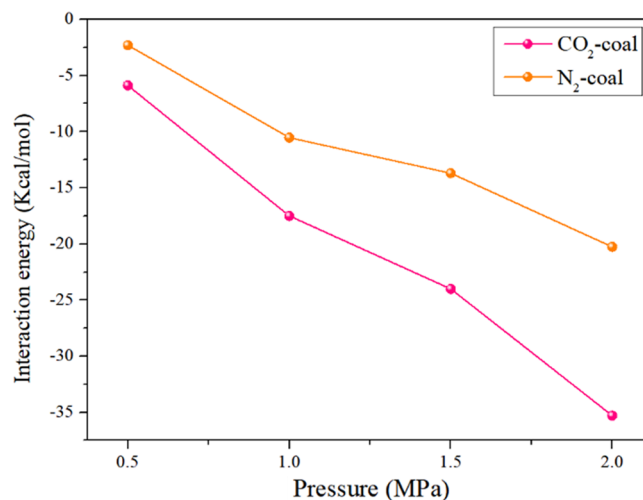


Figure 13. Interaction energies of CO_2 , N_2 , and coal under different pressure conditions.

gradually accumulates and will have a certain resistance to the entry of liquid.

Figure 14 shows the variation process of the contact angle at the molecular scale. With a certain gas pressure gradient, the

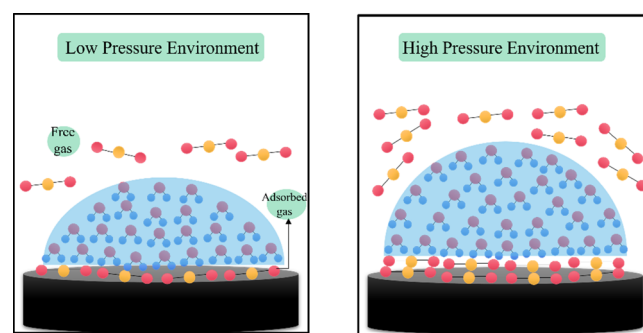


Figure 14. Schematic diagram of coal–water contact angle variation under different gas environments.

gas is gradually adsorbed on the surface of the coal and exists in the form of a “gas film”³⁶ and this creates an additional barrier to coal–water contact. The higher the pressure, the multi-molecular layer adsorption of the gas will result in a thicker “gas film”, thus more deeply impede the effect of coal–water wetting.

5. CONCLUSIONS

- (1) The contact angle test results in different gas environments show that the higher the pressure, the higher the contact angle, and the values are $\text{CO}_2 > \text{N}_2 > \text{He}$ in descending order.
- (2) Based on the experimental results of XRD, FTIR, and ^{13}C NMR, the SP coal macromolecular model was constructed. The results of the molecular dynamics simulation showed that the adsorptive gases, such as CO_2 and N_2 would be pre-adsorbed in coal, occupying the adsorption sites, and competing with the subsequent entry of water molecules. In addition, the stronger gas adsorption capacity is able to occupy more adsorption sites and thus inhibit the water molecule adsorption.
- (3) When coal molecules pre-adsorb different gas molecules, the surface free energy of coal will be reduced and the system becomes more stable, thus weakening the adsorption ability of coal to water molecules. The more gas is adsorbed, the more the surface free energy of coal is reduced, and the worse the coal wettability.
- (4) The pressure has a crucial influence on coal wettability. The higher the gas pressure, the worse the coal-water wettability. The effect of pressure on coal wettability is mainly due to the increase of gas density in coal pores caused by the increase of resistance of water molecules to enter. The increase in air pressure will promote the enhancement of coal-gas molecule binding ability. Thus, it weakens the adsorption capacity of coal on water molecules. The research can provide theoretical support for water injection in gas-bearing coal seams.

■ AUTHOR INFORMATION

Corresponding Author

Leilei Si – School of Safety Science and Engineering and State Key Laboratory Cultivation Base for Gas Geology and Gas Control, Henan Polytechnic University, Jiaozuo, Henan 454003, China; orcid.org/0000-0001-5351-5612; Email: si_leilei@hpu.edu.cn

Authors

Nan Ding – School of Safety Science and Engineering and State Key Laboratory Cultivation Base for Gas Geology and Gas Control, Henan Polytechnic University, Jiaozuo, Henan 454003, China

Jianping Wei – School of Safety Science and Engineering and State Key Laboratory Cultivation Base for Gas Geology and Gas Control, Henan Polytechnic University, Jiaozuo, Henan 454003, China

Wan Jiang – School of Safety Science and Engineering and State Key Laboratory Cultivation Base for Gas Geology and Gas Control, Henan Polytechnic University, Jiaozuo, Henan 454003, China

Jian Zhang – School of Safety Science and Engineering and State Key Laboratory Cultivation Base for Gas Geology and Gas Control, Henan Polytechnic University, Jiaozuo, Henan 454003, China

Yong Liu – School of Safety Science and Engineering and State Key Laboratory Cultivation Base for Gas Geology and Gas Control, Henan Polytechnic University, Jiaozuo, Henan 454003, China

Complete contact information is available at:
<https://pubs.acs.org/10.1021/acsomega.3c02645>

Author Contributions

N.D.: writing-original draft and supervision. L.S.: data curation, methodology, and software. J.W.: review and editing. W.J.: software. J.Z.: data curation. Y.L.: software.

Notes

The authors declare no competing financial interest.

■ ACKNOWLEDGMENTS

This study was supported by the program for National Natural Science Foundation of China (52004083, 52274193, 52174174), Outstanding Youth Fund of Henan Polytechnic University (J2023-1), the Plan of Key Scientific Research Projects of Colleges and Universities in Henan Province (21A440002).

■ REFERENCES

- (1) Liu, W.; Xu, X.; Han, J.; Wang, B.; Li, Z.; Yan, Y. Trend model and key technologies of coal mine methane emission reduction aiming for the carbon neutrality. *J. China Coal Soc.* **2022**, *47*, 470–479.
- (2) Pan, Y. Integrated study on compound dynamic disaster of coal-gas outburst and rockburst. *J. China Coal Soc.* **2016**, *41*, 105–112.
- (3) Guo, H.; Su, X. Research on the mechanism of gas emission inhibition in water-flooding coal seam. *J. China Coal Soc.* **2010**, *35*, 928–931.
- (4) Wei, J.; Wei, L.; Wang, D. Experimental study of moisture content influences on permeability of coal containing gas. *J. China Coal Soc.* **2014**, *39*, 97–103.
- (5) Yang, H.; Liu, Z.; Zhao, D.; Lv, J.; Yang, W. Insights into the fluid wetting law and fractal characteristics of coal particles during water injection based on nuclear magnetic resonance. *Chaos, Solitons Fractals* **2022**, *159*, No. 112109.
- (6) Zhou, Y.; Zhang, R.; Huang, J.; Li, Z.; Chen, Z.; Zhao, Z.; et al. Influence of alkaline solution injection for wettability and permeability of coal with CO_2 injection. *Energy* **2020**, *202*, No. 117799.
- (7) Cheng, W.; Xue, J.; Zhou, G.; Nie, W.; Wen, J. Research on the relationship between bituminous coal dust wettability and inorganic mineral content. *J. China Univ. Min. Technol.* **2016**, *45*, 462–468.
- (8) Li, J.; Li, K. Influence factors of coal surface wettability. *J. China Coal Soc.* **2016**, *41*, 448–453.
- (9) Zhang, C.; Wang, X.; Li, S.; Jiang, B.; Zhai, C.; Zhu, C.; et al. Development and application of a new compound wetting agent for coal seam water infusion. *Fuel* **2022**, *314*, No. 122767.
- (10) Zhao, Z.; Chang, P.; Xu, G.; Xie, Q.; Ghosh, A. Comparison of static tests and dynamic tests for coal dust surfactants evaluation: a review. *Fuel* **2022**, *330*, No. 125625.
- (11) Yao, Y.; Liu, D. Petrophysics and fluid properties characterizations of coalbed methane reservoir by using NMR relaxation time analysis. *Coal Sci. Technol.* **2016**, *44*, 14–22.
- (12) Chen, J.; Yao, Y.; Sun, X.; Xie, S.; Guo, W. Research on influences of carbon dioxide and helium on wettability of low rank coal. *Coal Sci. Technol.* **2015**, *43*, 129–134.
- (13) Chaturvedi, T.; Schembre, J. M.; Kovscek, A. R. Spontaneous imbibition and wettability characteristics of powder river basin coal. *Int. J. Coal Geol.* **2009**, *77*, 34–42.
- (14) Ibrahim, A. F.; Nasr-El-Din, H. A. Effect of water salinity on coal wettability during CO_2 sequestration in coal seams. *Energy Fuels* **2016**, *30*, 7532.
- (15) Wei, J.; Wang, H.; Si, L.; Xi, Y. Characteristics of coal-water solid-liquid contact in gas atmosphere. *J. China Coal Soc.* **2022**, *47*, 323–332.
- (16) Yi, Z.; Yuannan, Z.; Bingyou, J.; Guofeng, Y.; Bo, R.; Changfei, Y.; et al. Experimental study on the influence of acid fracturing fluid on coal wettability. *Fuel* **2023**, *343*, No. 127965.
- (17) Jian, G.; Deming, W.; Zhongmin, X.; Ya-Nan, W.; Kang, Z.; Xiaolong, Z.; et al. Experimental and molecular dynamics investigations of the effects of ionic surfactants on the wettability of low-rank coal. *Energy* **2023**, *271*, No. 127012.

- (18) Chai, S.; Zeng, Q. Molecular model construction and structural characteristics analysis of Wucuiwan coal in Eastern Junggar Coalfield based on quantum chemistry theory. *J. China Coal Soc.* **2022**, *47*, 4504–4516.
- (19) Zhang, J.; Li, H.; Liu, Y.; Li, X.; Xie, J.; Dai, Z.; et al. Micro-wetting characteristics of coal dust and preliminary study on the development of dust suppressant in Pingdingshan mining area. *J. China Coal Soc.* **2021**, *46*, 812–825.
- (20) Cheng, W.; Xue, J.; Zhou, G.; Nie, W.; Liu, L. Study of coal dust wettability based on FTIR. *J. China Coal Soc.* **2014**, *39*, 2256–2262.
- (21) Lim, D. J.; Marks, N. A.; Rowles, M. R. Universal scherrer equation for graphene fragments. *Carbon* **2020**, *162*, 475.
- (22) Lu, G.; Wei, C.; Wang, J.; Meng, R.; Tamehe, L. S. Influence of pore structure and surface free energy on the contents of adsorbed and free methane in tectonically deformed coal. *Fuel* **2021**, *285*, No. 119087.
- (23) Si, L.; Wei, J.; Xi, Y.; Wang, H.; Wen, Z.; Li, B.; et al. The influence of long-time water intrusion on the mineral and pore structure of coal. *Fuel* **2021**, *290*, No. 119848.
- (24) Zhou, L.; Feng, Q.; Qin, Y. Thermodynamic analysis of competitive adsorption of CO₂ and CH₄ on coal matrix. *J. China Coal Soc.* **2011**, *36*, 1307–1311.
- (25) Jin, Z.; Wu, S.; Deng, C.; Dai, F. H₂O adsorption mechanism in coal basing on Monte Carlo method. *J. China Coal Soc.* **2017**, *42*, 2968–2974.
- (26) Xianfeng, L.; Xueqi, J.; Wei, L.; Baisheng, N.; Chengpeng, Z.; Dazhao, S. Mechanical strength and porosity changes of bituminous coal induced by supercritical CO₂ interactions: influence of saturation pressure. *Geoenergy Sci. Eng.* **2023**, *225*, No. 211691.
- (27) Zhongbei, L.; Ting, R.; Xiangchun, L.; Ming, Q.; Xiaohan, Y.; Lihai, T.; et al. Multi-scale pore fractal characteristics of differently ranked coal and its impact on gas adsorption. *Int. J. Min. Sci. Technol.* **2023**, *33*, 389.
- (28) Zhang, Z.; Ma, P. Experimental on moisture effects on the gas absorption speciality of different kinds of coal. *J. China Coal Soc.* **2008**, *33*, 144–147.
- (29) Leilei, S.; Nan, D.; Jianping, W.; Lianchao, S.; Lei, W.; Zhiwei, L.; et al. Gas-liquid competitive adsorption characteristics and coal wetting mechanism under different pre-adsorbed gas conditions. *Fuel* **2022**, *329*, No. 125441.
- (30) Huang, B.; Lu, W.; Chen, S.; Zhao, X. Experimental investigation of the functional mechanism of methane displacement by water in the coal. *Adsorpt. Sci. Technol.* **2020**, *38*, 376.
- (31) Si, L.; Zhang, H.; Wei, J.; Li, B.; Han, H. Modeling and experiment for effective diffusion coefficient of gas in water-saturated coal. *Fuel* **2021**, *284*, No. 118887.
- (32) Tao, Y.; Qi, L.; Xiaochun, L.; Haixiang, H.; Yongsheng, T.; Liang, X. Synergistic effects of CO₂ density and salinity on the wetting behavior of formation water on sandstone surfaces: molecular dynamics simulation. *J. Nat. Gas Sci. Eng.* **2022**, *105*, No. 104714.
- (33) Kang, C.; Xianfeng, L.; Baisheng, N.; Chengpeng, Z.; Dazhao, S.; Longkang, W.; et al. Mineral dissolution and pore alteration of coal induced by interactions with supercritical CO₂. *Energy* **2022**, *248*, No. 123627.
- (34) Tang, J.; Ma, Y.; Tian, H. Molecular simulation of methane adsorption amount in anthracite coal based on Monte Carlo method. *Prog. Geophys.* **2017**, *32*, 1823–1827.
- (35) Zarzor, A. Y. A.; Hamid, R.; Xiaomeng, X.; Yihuai, Z.; Mohammed, S.; Maxim, L.; et al. Coal wettability after CO₂ injection. *Energy Fuels* **2017**, *31*, 12376.
- (36) Zhang, L.; He, X.; Wang, E.; Liu, Z.; Ma, S. Study of Absorptive Characteristics of coal. *J. Taiyuan Univ. Technol.* **2001**, 449–451.